THE JOURNAL OF BIOLOGICAL CHEMISTRY VOL. 286, NO. 28, pp. 25224–25235, July 15, 2011

Plasma Membrane Aquaporin AqpZ Protein Is Essential for Glucose Metabolism during Photomixotrophic Growth of *Synechocystis* sp. PCC 6803*[S]

Received for publication, March 3, 2011, and in revised form, April 21, 2011 Published, JBC Papers in Press, May 10, 2011, DOI 10.1074/jbc.M111.236380

Masaro Akai[‡], Kiyoshi Onai[§], Miyako Kusano[¶], Mayuko Sato[¶], Henning Redestig[¶], Kiminori Toyooka[¶], Megumi Morishita[§], Hiroshi Miyake[‖], Akihiro Hazama[**], Vanessa Checchetto[‡‡], Ildikò Szabò[‡‡], Ken Matsuoka[¶§§], Kazuki Saito[¶¶¶], Masato Yasui[‖‖], Masahiro Ishiura[§], and Nobuyuki Uozumi[‡1]

From the [‡]Department of Biomolecular Engineering, Graduate School of Engineering, Tohoku University Aobayama 6-6-07, Sendai 980-8579, Japan, the [§]Center for Gene Research, Nagoya University, Nagoya 464-8602, Japan, the [¶]RIKEN Plant Science Center, Yokohama, Kanagawa 230-0045, Japan, the [‖]Graduate School of Bioagricultural Sciences, Nagoya University, Nagoya 464-8603, Japan, the [**]Department of Physiology, School of Medicine, Fukushima Medical University, Fukushima 960-1295, Japan, the [‡‡]Department of Biology, University of Padova, Padova 35121, Italy, the [§§]Laboratory of Plant Nutrition, Faculty of Agriculture, Kyushu University, Higashi-ku, Fukuoka 812-8581, Japan, the [¶¶]Graduate School of Pharmaceutical Sciences, Chiba University, Chiba 263-8522, Japan, and the [‖‖]Department of Pharmacology, School of Medicine, Keio University, Shinanomachi, Shinjyuku-ku, Tokyo 160-8582, Japan

The genome of *Synechocystis* PCC 6803 contains a single gene encoding an aquaporin, *aqpZ*. The AqpZ protein functioned as a water-permeable channel in the plasma membrane. However, the physiological importance of AqpZ in *Synechocystis* remains unclear. We found that growth in glucose-containing medium inhibited proper division of Δ*aqpZ* cells and led to cell death. Deletion of a gene encoding a glucose transporter in the Δ*aqpZ* background alleviated the glucose-mediated growth inhibition of the Δ*aqpZ* cells. The Δ*aqpZ* cells swelled more than the wild type after the addition of glucose, suggesting an increase in cytosolic osmolarity. This was accompanied by a down-regulation of the pentose phosphate pathway and concurrent glycogen accumulation. Metabolite profiling by GC/TOF-MS of wild-type and Δ*aqpZ* cells revealed a relative decrease of intermediates of the tricarboxylic acid cycle and certain amino acids in the mutant. The changed levels of metabolites may have been the cause for the observed decrease in growth rate of the Δ*aqpZ* cells along with decreased PSII activity at pH values ranging from 7.5 to 8.5. A mutant in *sll1961*, encoding a putative transcription factor, and a Δ*hik31* mutant, lacking a putative glucose-sensing kinase, both exhibited higher glucose sensitivity than the Δ*aqpZ* cells. Examination of protein expression indicated that *sll1961* functioned as a positive regulator of *aqpZ* gene expression but not as the only regulator. Overall, the Δ*aqpZ* cells showed defects in macronutrient metabolism, pH homeostasis, and cell division under photomixotrophic conditions, consistent with an essential role of AqpZ in glucose metabolism.

Since identification of the first aquaporin from red blood cells (1), genes encoding aquaporins have been found in both prokaryotic and eukaryotic cells. In animals, abundant major intrinsic protein isoforms are involved in a number of diseases and are known to have a role in the regulation of water homeostasis (2). In plants, aquaporins regulate water permeability and transport in response to external changes in water supply (3). The first aquaporin to be isolated from plant cells was the tonoplast intrinsic protein, γ-TIP (4). This finding established that aquaporins reside not only in the plasma membrane but also in endomembranes, presumably to coordinate water transport inside the cell. In *Synechocystis* sp. PCC 6803 (henceforth referred to as *Synechocystis*) a single copy gene encoding an aquaporin homolog, *aqpZ*, is present in the genome. The functional characteristics of AqpZ and its subcellular localization in *Synechocystis* have not been determined, although microarray experiments have identified a list of genes induced by hyperosmotic stress in both the wild type (WT) and a Δ*aqpZ* strain (5). Moreover, loss of aquaporins in microorganisms in general does not result in growth defects under a range of environmental conditions (6). Hence, the question as to the physiological role of aquaporins in microbial cells remains open.

In microorganisms, the best studied aquaporin is the AqpZ protein from *Escherichia coli*. The *aqpZ* null mutant forms smaller colonies and has reduced viability in medium with low osmolarity compared with the parental wild-type cells (7). However, another study failed to detect any growth defects of an *aqpZ* disruption mutant under any condition tested (8). Although wild-type *E. coli* cells have higher water permeability compared with an *aqpZ* null mutant, it has not been demonstrated that aquaporins are important for proper osmotic adjustment (9). Although the physiological relevance of *E. coli* AqpZ remains unclear, other functions of aquaporins that are related to specific ecological lifestyles or developmental stages have received increased attention (6, 10). Some aquaporin isoforms mediate permeation of glycerol, H_2O_2, CO_2, silicon, or boron in addition to water (11, 12). The range of specificities of aquaporins implies that they are involved in processes as

* This work was supported by MEXT and Japan Society for the Promotion of Science Grants-in-aid for Scientific Research 22020002 and 22380056 (to N. U.) and the Salt Science Research Foundation.

[S] The on-line version of this article (available at http://www.jbc.org) contains supplemental Figs. S1–S7.

[1] To whom correspondence should be addressed. Fax: 81-22-795-7293; E-mail: uozumi@biophy.che.tohoku.ac.jp.

diverse as nutrient acquisition, control of development, and growth and defense responses against environmental stress.

Cyanobacteria are prokaryotic microorganisms that perform oxygenic photosynthesis and are adapted to a regular cycle of light and dark periods, in which they are different from non-photosynthetic microorganisms. In most species of cyanobacteria, glycogen accumulated during the day serves as the predominant metabolic fuel at night. Glucose derived from glycogen or supplied exogenously is catabolized via the oxidative pentose phosphate pathway, glycolysis, and the tricarboxylic acid (TCA) cycle, leading to the production of ATP and carbon skeletons. A glucose-tolerant strain of the cyanobacterium *Synechocystis* has been isolated previously (13). These cells grow photoautotrophically under light conditions but are also capable of photomixotrophic growth or light-activated heterotrophic growth in glucose-supplemented media (14).

In the present study, we determined the membrane localization and investigated the physiological role of aquaporin AqpZ in *Synechocystis*. The addition of glucose to Δ*aqpZ* cells triggered structural aberrations and morphological abnormalities. Moreover, Δ*aqpZ* cells growing on medium containing glucose accumulated more glycogen, and their glucose catabolysis was down-regulated. These data suggest that AqpZ plays a crucial role in the regulation of glucose metabolism under photomixotrophic conditions. To our knowledge, this is the first evidence of a physiological role of AqpZ in addition to its role in the osmotic stress response.

EXPERIMENTAL PROCEDURES

Plasmid Construction—The *aqpZ* coding region of *Synechocystis slr2057* was amplified from genomic DNA by PCR using gene-specific primers (sense, 5′-CAGTAGATCTATGAAAAAGTACATTGCTG-3′; antisense, 5′-CAGTGCTAGCTCACTCTGCTTCGGGTTCG-3′). The resulting PCR product was cloned into the BglII and NheI sites of pXβG-ev1 (1). To create Myc-tagged AqpZ, another set of primers (sense, 5′-CATGGAATTCCATGAAAAAGTACATTGCTG-3′; antisense, 5′-CAGTGCTAGCTCACTCTGCTTCGGGTTCG-3′) was used to amplify the coding region of *aqpZ* from genomic DNA by PCR, and the resulting PCR product was cloned into the EcoRI and NheI sites of pXβG-ev1, placing it in frame with the N-terminal Myc tag contained in the vector. The correct frame was verified by sequencing. Myc-Y69 (AQP-3) from *C. elegans* and the human aquaporin hAQP1 were used as controls (1).

Expression in Xenopus Oocytes and Measurement of Water Permeability—Capped cRNAs were synthesized *in vitro* from XbaI-linearized pXβG-ev1 plasmids using the mMESSAGE mMACHINE T3 kit (Ambion, Austin, TX). Defolliculated *Xenopus laevis* oocytes were injected with 5 or 10 ng of cRNA or diethyl pyrocarbonate-treated water (1, 15). Injected oocytes were incubated for 2–3 days at 18 °C in 200 mosM modified Barth's solution (10 mM Tris-HCl (pH 7.6), 88 mM NaCl, 1 mM KCl, 2.4 mM $NaHCO_3$, 0.3 mM $Ca(NO_3)_2$, 0.4 mM $CaCl_2$, 0.8 mM $MgSO_4$). An oocyte swelling assay was used to determine the osmotic water permeability, P_f (1). Oocytes were transferred to modified Barth's solution diluted to 70 mosM with distilled water, and the time course of volume increase was monitored at room temperature by video microscopy with an on-line computer (16, 17). The relative volume (V/V_0) was calculated essentially as described by Preston *et al.* (1). The relative volume (V/V_0) was calculated from the area at the initial time (A_0) and after a time interval (At): $V/V_0 = (At/A_0)^{3/2}$. The coefficient of osmotic water permeability (P_f) was determined from the initial slope of the time course ($d(V/V_0)/dt$), initial oocyte volume ($V_0 = 9 \times 10^{-4}$ cm^3), initial oocyte surface area ($S = 0.045$ cm^2), and the molar volume of water ($V_w = 18$ cm^3/mol): $P_f = (V_0 \times d(V/V_0)/dt)/(S \times V_w \times (osM_{in} - osM_{out}))$.

Oocyte Immunofluorescence and Confocal Microscopy—Oocytes were incubated in fixing solution (80 mM Pipes, pH 6.8, 5 mM EGTA, 1 mM $MgCl_2$, 3.7% formaldehyde, 0.2% Triton X-100) at room temperature for 4 h, transferred to methanol at −20 °C for 24 h, equilibrated in PBS (3.2 mM Na_2HPO_4, 0.5 mM KH_2PO_4, 1.3 mM KCl, 135 mM NaCl, pH 7.4) at room temperature for 2 h, incubated in PBS with 100 mM $NaBH_4$ at room temperature for 24 h, and bisected with a razor blade (18). Fixed oocytes were blocked in PBS containing 2% BSA for 1 h at room temperature and then incubated at 4 °C with the anti-AqpZ antibody (see below) for 24 h followed by incubation with Alexa Fluor 488 goat anti-rabbit IgG in PBS containing 2% BSA for 24 h. Samples were mounted in Fluoromount-G (Southern Biotechnology Associates) and visualized with a PerkinElmer UltraView LCI confocal laser-scanning microscope.

Oocyte Membrane Extraction and Immunoblotting—For each sample, 10 oocytes were homogenized together by pipetting up and down in hypotonic lysis buffer (7.5 mM sodium phosphate, 1 mM EDTA, pH 7.5) containing a protease inhibitor mixture (Sigma-Aldrich) (19). The oocyte yolk was removed by discarding the pellet after a centrifugation at 735 × *g* and 4 °C for 10 min. The supernatant was then centrifuged at 200,000 × *g*, 4 °C, for 1 h. The pellet containing the oocyte membrane fraction was solubilized in buffer (50 mM Tris-HCl (pH 8.0), 50 mM NaCl, 50 mM EDTA-2Na, 10% (w/v) glycerol, and 2% SDS). Total protein content was determined by the bicinchoninic acid (BCA) assay method (Pierce). Equal amounts of protein were separated by SDS-PAGE on a 12% gel. Proteins were transferred to a polyvinylidene difluoride (PVDF) membrane, probed with either anti-AqpZ antibody (see below) or anti-Myc antibody (Santa Cruz Biotechnology, Inc., Santa Cruz, CA) followed by horseradish peroxidase-conjugated donkey anti-rabbit IgG (Amersham Biosciences). The enhanced chemiluminescence detection system (Amersham Biosciences) was used to visualize the immunoreactive proteins by exposure to x-ray films.

Isolation of Synechocystis Membranes—Thylakoid and plasma membrane fractions were prepared from *Synechocystis* cells as described previously (20, 21). An anti-AqpZ antibody was raised against two synthetic peptides with the sequences NH_2-GSNPLATNGFGDHS-COOH and NH_2-VLEDLGRPEPEAE-COOH (Operon, Tokyo, Japan). Polyclonal antibodies raised against the plasma membrane nitrate transporter NrtA (22) or against the thylakoid membrane proteins $NdhD_3$ and $NdhF_3$ (23, 24) were used to identify the *Synechocystis* plasma membrane, or thylakoid membrane fractions, respectively. Proteins were separated by SDS-PAGE on a 12.5 or 15% gel and then transferred to PVDF membranes. Membranes were incu-

bated for 1 h with the primary antibody (1:2000 in blocking buffer), followed by incubation for 30 min with the secondary antibody (horseradish peroxidase-conjugated goat anti-rabbit IgG (Amersham Biosciences; 1:1000)) and subsequently developed by ECL (Amersham Biosciences).

Immunolabeling and Electron Microscopy—*Synechocystis* cells grown to an OD_{730} of about 1.0 in BG11 medium were fixed with 50 mM phosphatase buffer containing 5% glutaraldehyde and 2% osmium tetroxide (pH 7.2). The samples were dehydrated through a graded acetone series and embedded in Spurr's resin and polymerized. Ultrathin sections were first labeled with AqpZ antiserum (1:20) in Tris-buffered saline and then with 12-nm colloidal gold particles coupled to goat anti-rabbit IgG. IgG was purified from the serum using the Melon™ Gel IgG spin purification kit (Pierce). The sections were stained with uranyl acetate followed by lead citrate solution and examined with a transmission electron microscope (H-7500, Hitachi).

Bacterial Strains and Culture Conditions—The GT (glucose tolerance) strain of *Synechocystis* sp. PCC 6803 and its derivatives were grown at 30 °C in BG11 medium (25) buffered with 20 mM TES[2]-KOH (pH 8.0) under aerobic conditions. Solid medium consisted of BG11 buffered at pH 8.0, with 1.5% agar, and 0.3% sodium thiosulfate. To test the effects of pH on growth of *Synechocystis* cells, a range of BG11 media were prepared by replacing TES buffer with MES buffer for pH 6.5, TES buffer for pH 7.0–8.0, Bicine buffer for pH 8.5, and CHES buffer for pH 9.0–10.0. Continuous illumination was provided by white fluorescent lamps (50 μmol of photons $m^{-2} s^{-1}$). For growth in the dark, culture vessels were wrapped with aluminum foil. For light-activated heterotrophic growth, BG11 plates supplemented with 5 mM glucose were incubated in the dark with a daily 15-min pulse of white light. Unless otherwise stated, cells were grown in volumes of 30 ml in flasks. In all experiments, cells grown in fresh BG11 media as precultures were transferred to BG11 (photoautotrophic growth condition) or BG11 containing 5 mM glucose (photomixotrophic growth condition) at an $OD_{730} = 0.05$.

Construction and Isolation of Mutants—In this study, several mutant strains (Δ*glcP* (*sll0771*), Δ*sll1961*, and Δ*aqpZ*/Δ*glcP*) were generated by homologous recombination using plasmids described elsewhere (21). The plasmids for disruption of the *glcP* or *sll1961* gene contained an insertion of a kanamycin (K_m^r) resistance cassette in the middle of the respective coding sequence. For reintegration of the *Synechocystis aqpZ* (*slr2057*) gene into the genome of the Δ*aqpZ* cells, the full-length coding sequence of *aqpZ* was amplified by PCR using an NdeI site-containing forward primer 5′-CAGTCATATGATGAAAAA-GTACATTGCTG-3′ and SalI site-containing reverse primer 5′-CAGTGTCGACTCACTCTGCTTCGGGTTCG-3′. The NdeI-SalI DNA fragment encoding AqpZ was inserted into the corresponding sites in p68TS4OxCm and integrated by homologous recombination into targeting site 4 of the chromosomal DNA of *Synechocystis* Δ*aqpZ* cells (21).

[2] The abbreviations used are: TES, 2-{[2-hydroxy-1,1-bis(hydroxymethyl)ethyl]amino}ethanesulfonic acid; Bicine, *N*,*N*-bis(2-hydroxyethyl)glycine; CHES, 2-(cyclohexylamino)ethanesulfonic acid.

Immunoblot Analysis—Cultures were grown to a cell density of $OD_{730} = 1.0$ and then transferred to fresh BG11 medium either with or without 5 mM glucose. The cells were lysed mechanically by vortexing with glass beads, and the proteins were separated by SDS-PAGE (12.5 or 15% gels) and then transferred to PVDF membranes. The membranes were probed with anti-AqpZ antibody and anti-OpcA antibody (26, 27). The membranes were incubated for 1 h with the primary antibody (1:2000 in blocking buffer) and then incubated for 30 min with the secondary antibody (horseradish peroxidase-conjugated goat anti-rabbit IgG (1:1000)) and subsequently subjected to chemiluminescence detection.

Assay of Glucose Uptake—Cells were collected at mid-exponential phase by centrifugation at 5,000 × *g* for 5 min and then resuspended in BG11 supplemented with 5 mM glucose at an OD_{730} of 0.05. Glucose uptake was determined by measuring the concentration of glucose in the medium enzymatically using the D-glucose kit (Roche Applied Science, R-Biopharm), following the manufacturer's instructions. Aliquots (200 μl) of the cultures were harvested every 12 h and centrifuged at 1,500 rpm for 2 min, followed by the determination of glucose concentration in the supernatant.

Optical and Transmission Electron Microscopy—Optical microscopy was performed with a microscope (Axioskop FL, Carl Zeiss, Gottingen) equipped with a high definition image capture camera (HC-1000, Fujix, Tokyo) as described previously (21, 28). The cell size was analyzed using ImageJ software (National Institutes of Health, Bethesda, MD) and beads of a defined diameter (3.005 ± 0.027 μm) as size standards. Cells grown under either photoautotrophic or photomixotrophic conditions were harvested. Cells were fixed in 4% paraformaldehyde and 2% glutaraldehyde in 100 mM cacodylate buffer (pH 7.2) and then postfixed in 1% osmium tetroxide in 50 mM cacodylate buffer. Samples were dehydrated through a graded methanol series, then embedded in Epon812 resin (28). The ultrathin sections were stained with uranyl acetate followed by lead citrate solution and examined with a 1010 transmission electron microscope (JEOL) at 80 kV (28).

Analysis of Cell Size Distribution—Cell size distribution was measured using a particle size distribution analyzer (CDA-1000X, Sysmex). Samples (100 μl) were taken from the cultures at the indicated intervals and diluted 100–500 times with modified physiological saline (0.45% sodium chloride, 144 mOSM) prior to performing the measurements.

Determination of Glycogen Content—Analysis of the intracellular glycogen content was performed as described elsewhere (29). The glucose produced by acid hydrolysis was quantified using a colorimetric assay (30).

E. coli Mutants and Growth Conditions—Deletion of chromosomal genes in *E. coli* was performed as described previously (31). *E. coli* MA02 (*glpF*::*km*) and *E. coli* MA03 (*aqpZ*::*cm*/*glpF*::*km*) were generated from the *E. coli* K-12 W3110 strain using the following primer sets: for aqpZ (JW0859) gene disruption, primers ΔEcAqpZ-PS1 (5′-CTATAAAACGACC-ATATTTTTCACAGGGTCAATTTTTAATTGTGGTGGA-TGTGTAGGCTGGAGCTGCTTC-3′) and ΔEcAqpZ-PS2 (5′-AACAACATCTTAAAAAAAGGCCTGACATTACGC-CAGGCCTTCTGCGTTAACATATGAATATCCTCCTT-

AGT-3′); for *glpF* (JW3898) gene disruption, primers ΔEcGlpF-PS1 (5′-GTCCGTGACTTTCACGCATACAACAAACATT-AACTCTTCAGGATCCGATTGTGTAGGCTGGAGCTGC-TTC-3′) and ΔEcGlpF-PS2 (5′-GCGCAACGATATATTTTT-TTTCAGTCATGTTTAATTGTCCCGTAGTCATACATA-TGAATATCCTCCTTAGT-3′). We removed the kanamycin and chloramphenicol resistance genes from *E. coli* MA02 and *E. coli* MA03 to generate strains MA05 (*glpF*$^-$) and MA06 (*aqpZ*$^-$/*glpF*$^-$) using the FLP-mediated recombination method (31). Bacterial strains were routinely plated on LB or M9 agar medium containing 50 mg/liter ampicillin. For overnight liquid cultures, bacterial strains were grown aerobically at 30 °C in M9 modified minimal medium with 0.2% casamino acids, 100 mg/liter ampicillin, and 10 mM maltose. Growth was monitored by measuring the A_{600} of the cultures in M9 modified medium supplemented with 2 mM glycerol (32).

Metabolite Profiling—Cultures were harvested by centrifugation at 15,000 × *g* at 4 °C for 2 min at the times indicated and washed twice with 1 ml of ice-cold distilled water to remove dead cells, and then cell pellets were frozen in liquid nitrogen. Each sample was extracted, derivatized, and analyzed by gas chromatography-time-of-flight mass spectrometry (GC/TOF-MS) as described (33–36). We used lyophilized samples for analysis. Each sample was prepared using 2 mg, dry weight, of cells for GC/TOF-MS analysis. Finally, 22 μg of fresh weight of the derivatized extract was injected into the GC/TOF-MS. Nonprocessed data were exported to the netCDF format using ChormaTOF software (version 3.22, Leco) for further data analysis. The raw data were processed using a custom script as described by Jonsson *et al.* (33, 34) to perform base-line correction, alignment, and peak deconvolution. Metabolites were identified by comparing their mass spectrum and retention time index with those generated for reference compounds analyzed on our instrumentation as well as those in the MS and retention time index libraries in the Golm Metabolome Database (37, 38).

Analysis of Metabolite Data—Analytical bias in metabolite measurements was controlled using cross-contribution-compensating multiple standard normalization (39) with 16 internal standard peaks. Metabolite peaks with more than 30% missing values were removed. Analysis of variance for examining correlation with glycogen levels and cell diameter was fitted for each metabolite. The formula for examining correlation with duration of culture, glycogen content, and cell diameter is shown in Fig. 8*A*. Model parameters were calculated using LIMMA (40) for the statistical environment R project (see the R Project site on the World Wide Web). *p* values were false discovery rate-adjusted to correct for multiple testing. The model used for studying the effect of genotype, *g*, glycogen level, *d*, and cell diameter, *p*, on the estimated level, *m*, of metabolite *i* in sample *j* was as follows,

$$m_{i,j} = \beta_i + g_{i,j} + d_{i,j} + p_{i,j} + g{:}d_{i,j} + g{:}p_{i,j} + \epsilon_{i,j} \quad \text{(Eq. 1)}$$

where *g*:*d* and *g*:*p* are the interactions between genotype and glycogen level and between genotype and cell diameter, respectively, β is the intercept, and ϵ is the error. We furthermore considered the following,

$$m_{i,j} = \beta_i + a_{i,j} + a^2{}_{i,j} + a{:}g_{i,j} + a^2{:}g_{i,j} + \epsilon_{i,j} \quad \text{(Eq. 2)}$$

to examine interaction between the same metabolite levels and the duration of culture *a*.

Oxygen Evolution Measurements—Cells grown under photoautotrophic or photomixotrophic conditions for 5 days were harvested by centrifugation at 5,000 × *g* at room temperature and resuspended in 20 mM TES buffer, pH 8.0, at an OD_{730} = 1.0. Cell suspensions were illuminated with white light at 1000 μmol of photon m^{-2} s^{-1}, and oxygen evolution was measured using a Clark-type electrode at 25 °C. For the determination of whole chain photosynthetic electron transport activities, cell suspensions were supplemented with 2 mM sodium bicarbonate. PS-II-mediated electron transport activities were measured in the presence of 1 mM 1,4-benzoquinone and 0.8 mM $K_3Fe(CN)_6$ in the cell suspension (41).

RESULTS

AqpZ-mediated Water Transport Was Insensitive to Inhibition by Mercury in Xenopus Oocytes—In order to evaluate its water transport activity, *Synechocystis* AqpZ was expressed in *Xenopus* oocytes. Correct expression of wild-type AqpZ or a Myc-tagged version in this system was confirmed by Western blot using either an antibody generated against *Synechocystis* AqpZ (see "Experimental Procedures") or an anti-Myc epitope antibody. Both proteins, wild-type AqpZ and Myc-tagged AqpZ, were detected in protein extracts of oocytes expressing the respective protein (Fig. 1*A*, *left*). Myc-tagged *C. elegans* aquaporin (Myc-Y69) was used as a positive control (Fig. 1*A*, *right*). The specificity of the anti-AqpZ antibody was also confirmed in this experiment. Confocal microscopy of immunolabeled oocytes showed that AqpZ was localized to the oocyte plasma membrane (Fig. 1*B*). Oocyte swelling assays were performed to measure AqpZ activity. Oocytes expressing either wild-type AqpZ or the Myc-tagged version exhibited a significant increase in osmotic water permeability (P_f) when compared with water-injected cells (Fig. 1, *C* and *D*). This indicated that *Synechocystis* AqpZ conferred water permeability.

AqpZ Is Localized to the Plasma Membrane—Fractions of plasma and thylakoid membranes were prepared by sucrose density gradient fractionation followed by aqueous polymer two-phase partitioning (20, 21, 24). As shown in Fig. 2*A*, a single protein band of the corresponding molecular mass (25.5 kDa) of AqpZ was detected by Western blot in the plasma membrane fraction, which was identified by the presence of the plasma membrane marker protein NrtA (22). No AqpZ protein was detected in the thylakoid membrane fraction, which was identified by the presence of $NdhD_3$ and $NdhF_3$ (23, 24). In addition, the membrane localization of the AqpZ protein was determined by immunogold labeling followed by electron microscopy. A cross-section of *Synechocystis* wild-type cells grown under non-stress conditions showed gold particles decorating the plasma membrane when incubated with the AqpZ antiserum (Fig. 2*B*). Only a small amount of the label was found in other locations. Control experiments with the Δ*aqpZ* strain did not show any significant labeling (supplemental Fig. S1). These results indicate that AqpZ was primarily localized in the plasma membrane of *Synechocystis*.

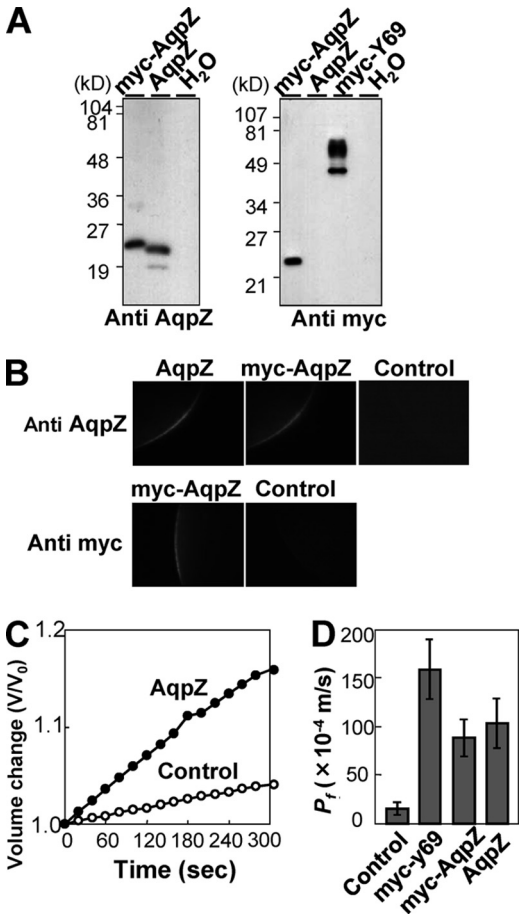

FIGURE 1. **Expression of *Synechocystis* AqpZ in oocytes.** *A*, immunoblotting of isolated membrane fractions from oocytes injected with water or expressing *Synechocystis* AqpZ, Myc-AqpZ, or Myc-tagged *C. elegans* aquaporin (Myc-Y69). Blots were probed with either anti-AqpZ (*left*) or anti-Myc antibodies (*right*). *B*, confocal microscopy images of oocytes injected with water (control) or expressing *Synechocystis* AqpZ or Myc-AqpZ. Oocytes were immunolabeled with anti-AqpZ antibodies (*top row*) or anti-Myc antibodies (*bottom row*) followed by an Alexa Fluor 488-conjugated secondary antibody. *C*, time-dependent osmotic swelling of water-injected oocytes and oocytes expressing *Synechocystis* AqpZ. *D*, osmotic water permeability (P_f) of *Synechocystis* AqpZ, Myc-AqpZ, or *C. elegans* Myc-Y69 expressed in *Xenopus* oocytes. Osmotic swelling assays were performed at 20 °C (mean ± S.D. (*error bars*), $n = 6–7$).

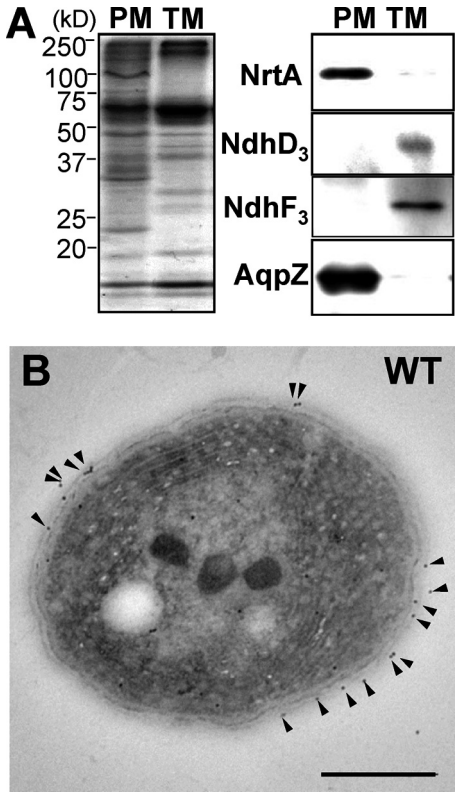

FIGURE 2. **Membrane localization of AqpZ in *Synechocystis*.** *A*, plasma membrane localization of AqpZ. Plasma membranes (*PM*) and thylakoid membranes (*TM*) were isolated by sucrose density fractionation followed by aqueous polymer two-phase partitioning. Shown are Coomassie Brilliant Blue staining (*left*) and immunoblotting (*right*) of the plasma membrane and the thylakoid membrane fractions from wild-type *Synechocystis*. NrtA (marker for the plasma membrane fraction) and $NdhD_3$ and $NdhF_3$ (markers for the thylakoid membrane fraction) were detected on Western blots using the corresponding antibodies. *B*, cross-section of *Synechocystis* wild-type cell immunolabeled using an anti-AqpZ antibody. AqpZ protein, indicated by the presence of gold particles (*arrowheads*), was localized in the plasma membrane. *Bar*, 500 nm.

Synechocystis Cells Lacking the Aquaporin AqpZ Were More Sensitive to Glucose in the Medium—When a glucose-tolerant wild-type strain of *Synechocystis* PCC 6803 and the aquaporin-deficient mutant, Δ*aqpZ*, derived from it were grown on BG11 plates in the absence of glucose, both grew equally well (Fig. 3*A*, *left*). However, the addition of 5 mM glucose to the BG11 medium strongly inhibited the growth of the Δ*aqpZ* strain (Fig. 3*A*, *right*). To confirm that lack of AqpZ was the reason for this sensitivity of Δ*aqpZ* cells to glucose, we reintroduced the *aqpZ* gene into a neutral site of the Δ*aqpZ* genome. The complementation construct consisted of *aqpZ* under control of the *trc* promoter, the resulting cells were designated +*aqpZ*. By using antibodies against AqpZ, we confirmed the presence of AqpZ protein in extracts from +*aqpZ* cells and the absence of AqpZ protein in extracts from Δ*aqpZ* cells (Fig. 3*B*). The complemented cells were able to grow on glucose medium as well as the wild type, whereas the Δ*aqpZ* cells did not grow (Fig. 3*C*). As a control and to exclude the possibility that the growth inhibition was caused by the change in osmolarity due to the addition of 5 mM glucose, we added sorbitol or L-glucose at the same concentration instead of glucose to the cells (Fig. 3*C* and supplemental Fig. S2). Only glucose caused growth inhibition of the Δ*aqpZ* cells. *Synechocystis* wild-type cells are able to grow heterotrophically in the dark if provided with a short pulse of white light in the presence of glucose (14). We examined the growth of Δ*aqpZ* cells under these heterotrophic conditions. An aliquot of a mid-logarithmic phase culture of either wild-type or Δ*aqpZ* cells grown on medium without glucose in the light was spotted onto solid BG11 plates with or without 5 mM glucose (Fig. 3*D*) and grown in the dark. In contrast to the wild-type cells, Δ*aqpZ* cells were incapable of growing on medium containing 5 mM glucose in the dark (Fig. 3*D*). Similar to this, after 48 h of growth in liquid medium with glucose in the light, the growth rate of Δ*aqpZ* cells was much slower than that of wild-type cells (Fig. 3*E*). These results indicate that loss of *aqpZ* caused hypersensitivity to glucose and that Δ*aqpZ* cells were unable to effectively use glucose as a carbon source for growth.

We observed individual *Synechocystis* cells grown in liquid medium with glucose using phase-contrast imaging. The number of dark cells was higher than the number of bright cells in the Δ*aqpZ* culture compared with the wild type (Fig. 4, *A* and

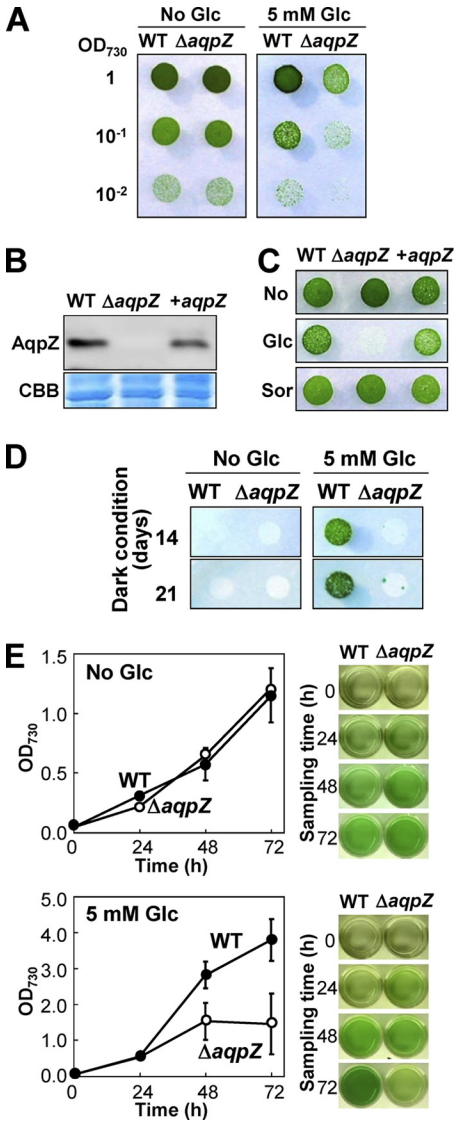

FIGURE 3. **Phenotype of the *aqpZ* mutants.** *A*, WT or Δ*aqpZ* cells grown to mid-exponential phase were spotted onto BG11 solid medium without (*left*) or with 5 mM glucose (*right*). Each spot consisted of 5 μl of liquid culture diluted to an OD_{730} of 1, 0.1, or 0.01, as indicated. Plates were maintained at 30 °C, 50 μmol of photons m^{-2} s^{-1}. Plates were photographed at 5 days after inoculation. *B*, amount of AqpZ protein in WT cells, Δ*aqpZ* cells, or Δ*aqpZ* cells complemented with the *aqpZ* gene (+*aqpZ*). Blots were probed with antiserum to AqpZ (*top*). Total protein (*CBB*) served as a loading control (*bottom*). *C*, growth of WT cells, Δ*aqpZ* cells, and +*aqpZ* cells on solid medium without an addition (*top*), with 5 mM glucose (*middle*), or with 5 mM sorbitol (*bottom*). *D*, WT or Δ*aqpZ* cells grown to mid-exponential phase were spotted onto solid medium without (*left*) or with 5 mM glucose (*right*). Each spot consisted of 5 μl of culture diluted to an OD_{730} of 1.0. The plates were incubated in the dark except for a short exposure to light (15 min each day) and photographed at days 14 and 21. *E*, growth curves (*left*) of WT (*filled circles*) and Δ*aqpZ* cells (*open circles*) in liquid medium without (*top*) and with 5 mM glucose (*bottom*) grown in the light. An aliquot of the cultures taken at the times indicated is shown on the *right*. Data and *error bars* (S.D.) correspond to the results of at least five independent experiments.

B). Those cells appearing dark using phase-contrast microscopy did not show autofluorescence under UV light (Fig. 4, *C* and *D*), indicating that they lacked chlorophyll. Based on these results, dark cells were considered to be dead cells. After growth for 48 or 72 h, the number of dark cells in cultures of the Δ*aqpZ* strain was much higher than in wild-type cultures (Fig. 4*E*). These results showed that AqpZ is essential for survival of *Synechocystis* under photomixotrophic conditions.

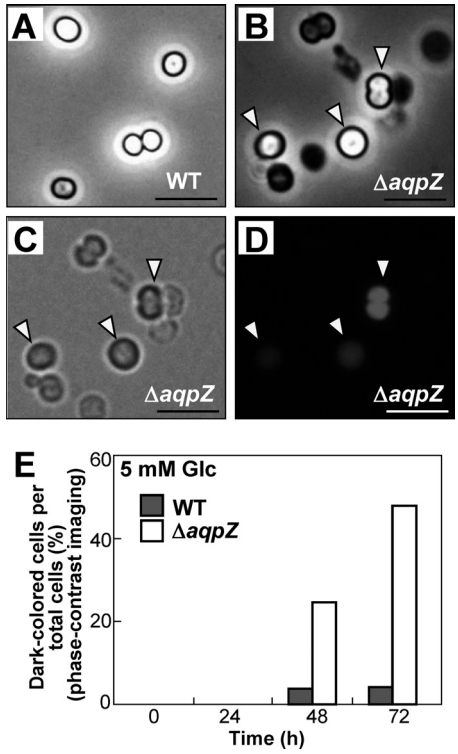

FIGURE 4. **Effects of glucose on the viability of Δ*aqpZ* cells.** *A–D*, WT and Δ*aqpZ* cells were cultured in liquid medium supplemented with 5 mM glucose (*Glc*) in the light. Shown are phase-contrast micrographs of WT (*A*) and Δ*aqpZ* cells (*B–D*). The Δ*aqpZ* cells in *B* were continuously monitored using bright field (*C*) and fluorescence microscopy (*D*). Cells shown were photographed at 72 h. The *arrows* indicate cells showing chlorophyll autofluorescence. *Bars*, 10 μm. *E*, percentage of the number of dark cells, determined using phase-contrast imaging in cultures grown in medium containing 5 mM glucose for the times indicated.

Deletion of aqpZ Resulted in an Increase in Cell Volume in the Presence of Glucose—While performing the microscopic observations shown in Fig. 4, we noticed a difference in size and morphology between the Δ*aqpZ* and the wild-type cells. We therefore compared wild-type and Δ*aqpZ* cells during incubation with or without 5 mM glucose under the microscope (Fig. 5, *A–D*). There was no significant difference in the size of wild-type and Δ*aqpZ* cells grown in liquid medium without glucose (Fig. 5, *A* and *B*). In contrast, after 48 h of growth on medium containing 5 mM glucose, both wild-type and Δ*aqpZ* cells became larger (Fig. 5, *C* and *D*). However, the diameter of the Δ*aqpZ* cells increased more than that of the wild-type cells (Fig. 5, *C* and *D*). The distribution of cell sizes of the wild type, Δ*aqpZ*, and cells lacking the glucose uptake transporter GlcP (Δ*glcP*) was evaluated over the course of 72 h using a particle counter (Fig. 5, *E–H*). The size distribution of wild-type, Δ*aqpZ*, and Δ*glcP* cells was similar when cells were grown without glucose (Fig. 5, *E* and *F*). After 24 h of incubation in the presence of 5 mM glucose, Δ*aqpZ* cells were larger than the wild-type cells. The size of the Δ*glcP* cells remained largely unchanged over the course of the experiment (Fig. 5, *G* and *H*). In the Δ*aqpZ* cell culture, a significant number of small cells (less than 1.5 mm in diameter) were observed after 48 h; these were most likely dead cells.

Cell Division Was Affected in ΔaqpZ Cells Grown in the Presence of Glucose—To assess the effects of glucose on cell morphology in Δ*aqpZ* cells, we examined the cells by transmission

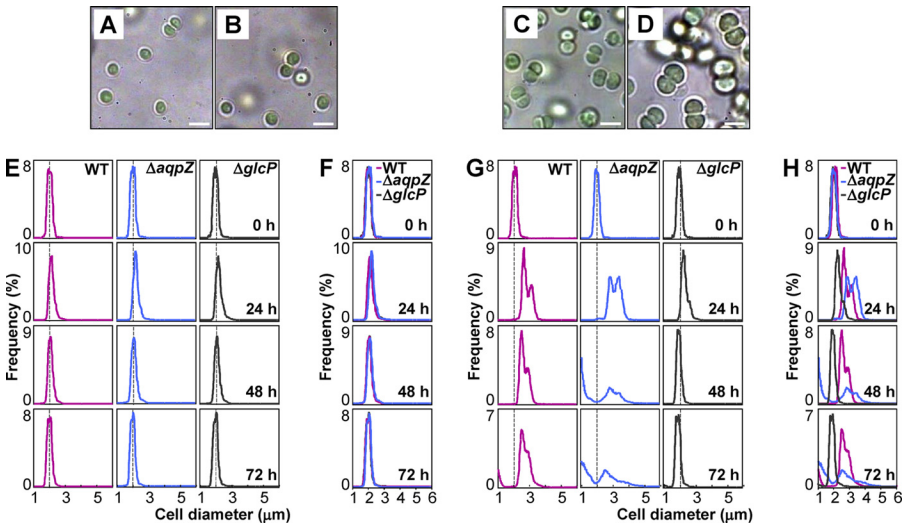

FIGURE 5. **Effects of glucose on the size distribution of *Synechocystis* cells.** *A–D*, WT and Δ*aqpZ* cells were grown under photoautotrophic or photomixotrophic (5 mM glucose) conditions. *A*, WT cells; *B*, Δ*aqpZ* cells; *C*, WT cells with 5 mM glucose; *D*, Δ*aqpZ* cells with 5 mM glucose. Cells were photographed at 48 h. *Bars*, 3 μm. *E–H*, WT, Δ*aqpZ* cells and Δ*glcP* cells were cultured in medium without (*E* and *F*) or with 5 mM glucose (*G* and *H*), and the cell sizes were determined by a particle counter. *Vertical dashed lines* in *E* and *G*, 2 μm in diameter of the cells. WT, Δ*aqpZ*, and Δ*glcP* cells are indicated by *red*, *blue*, and *gray lines*, respectively. *F* and *H*, overlays of the distributions shown in *E* and *G*, respectively.

electron microscopy. When both wild-type and Δ*aqpZ* cells were cultured in medium without glucose, their appearance was similar (Fig. 6, *A* and *E*). After incubation in liquid medium with glucose for 24 h, glycogen granules (white spots) were visible in sections of both wild-type and Δ*aqpZ* cells to a similar extent (Fig. 6, *B* and *F*). However, at 48 and 72 h, a number of Δ*aqpZ* cells containing glycogen granules showed dramatic changes compared with the wild type (Fig. 6, *G–I*). The structure of the thylakoid membranes in these Δ*aqpZ* cells was disordered, and oval-shaped cells containing bodies of high electron density were observed (Fig. 6, *I* and *J*). Fig. 6, *G–J*, shows the unusual appearance of these cells that also were unable to complete cell division. These structural aberrations and morphological abnormalities of Δ*aqpZ* cells were correlated with the presence of glucose in the medium.

Glucose Uptake Is Required for Glucose-induced Growth Inhibition of Δ*aqpZ Cells*—To examine whether Δ*aqpZ* cells were sensitive to intracellular or extracellular glucose, we studied the effect of deletion of the glucose uptake transporter, GlcP (42–44). Consistent with previously reported results, the Δ*glcP* mutant showed strongly reduced glucose uptake from the medium (Fig. 7*A*). When GlcP was deleted in the Δ*aqpZ* background (Δ*glcP*/Δ*aqpZ* mutant), these cells were no longer sensitive to glucose (Fig. 7*B*). Next, glucose analogs were tested to assess the cause of glucose toxicity in Δ*aqpZ* cells. L-Glucose (an enantiomer of glucose, which is very poorly transported into cells), 3-*o*-methyl-glucose (a glucose analog, which can be taken up into the cell but not phosphorylated by hexokinase), 2-deoxyglucose (which is phosphorylated by hexokinase but inhibits the production of glucose 6-phosphate, NADPH, and ATP), or fructose was added to solid media and growth was tested. Unlike glucose, none of the analogs resulted in a significant difference in growth between wild-type and Δ*aqpZ* cells, either on solid (Fig. 7*C*) or in liquid media (data not shown) (44). These data indicated that there is no difference in glucose uptake or hexokinase activity between the wild-type and Δ*aqpZ* cells.

The Activity of the Pentose Phosphate Pathway was Decreased in Δ*aqpZ Cells*—The expression of genes encoding enzymes in the glycolytic and the pentose phosphate pathways has been studied under various nutrient conditions (29, 44–50). Following its uptake into the cell, glucose is converted to glucose 6-phosphate by glucokinase, and glucose 6-phosphate is then further metabolized by glucose 6-phosphate dehydrogenase, an enzyme belonging to the pentose phosphate pathway. In *Synechocystis*, the OpcA protein is required for glucose-6-phosphate dehydrogenase activity (26, 27). Changes in the amount of OpcA protein in response to the addition of glucose to the medium were determined by immunological analysis (Fig. 8, *A* and *B*). Expression of OpcA protein was induced by glucose after 48 h (Fig. 8, *A* and *B*). However, the level of induction of OpcA protein in Δ*aqpZ* was approximately half as high as that in the wild type (Fig. 8, *A* and *B*). This indicates that the *aqpZ* mutation inhibited the glucose-mediated activation of the pentose phosphate pathway.

Δ*aqpZ Cells Contained More Glycogen*—The decrease in induction of OpcA protein in Δ*aqpZ* cells in response to glucose (Fig. 8) and the existence of glycogen granules in the cells (Fig. 6) suggested that glucose catabolism was decreased in these cells as well. We therefore hypothesized that the cells may convert excess glucose to glycogen in order to prevent an increase in intracellular osmolarity. The glycogen content of wild-type and Δ*aqpZ* cells during log phase was the same before the addition of glucose (0 h in Fig. 9). After the addition of glucose to the medium, the amount of glycogen reached its peak at 48 h in the wild type and then decreased again. The Δ*aqpZ* cells accumulated significantly more glycogen over the course of the experiment than the wild type, and no decrease in glycogen content was seen at 72 h (Fig. 9), at which point the mutant contained 5.6 times more glycogen than the wild type at 0 h.

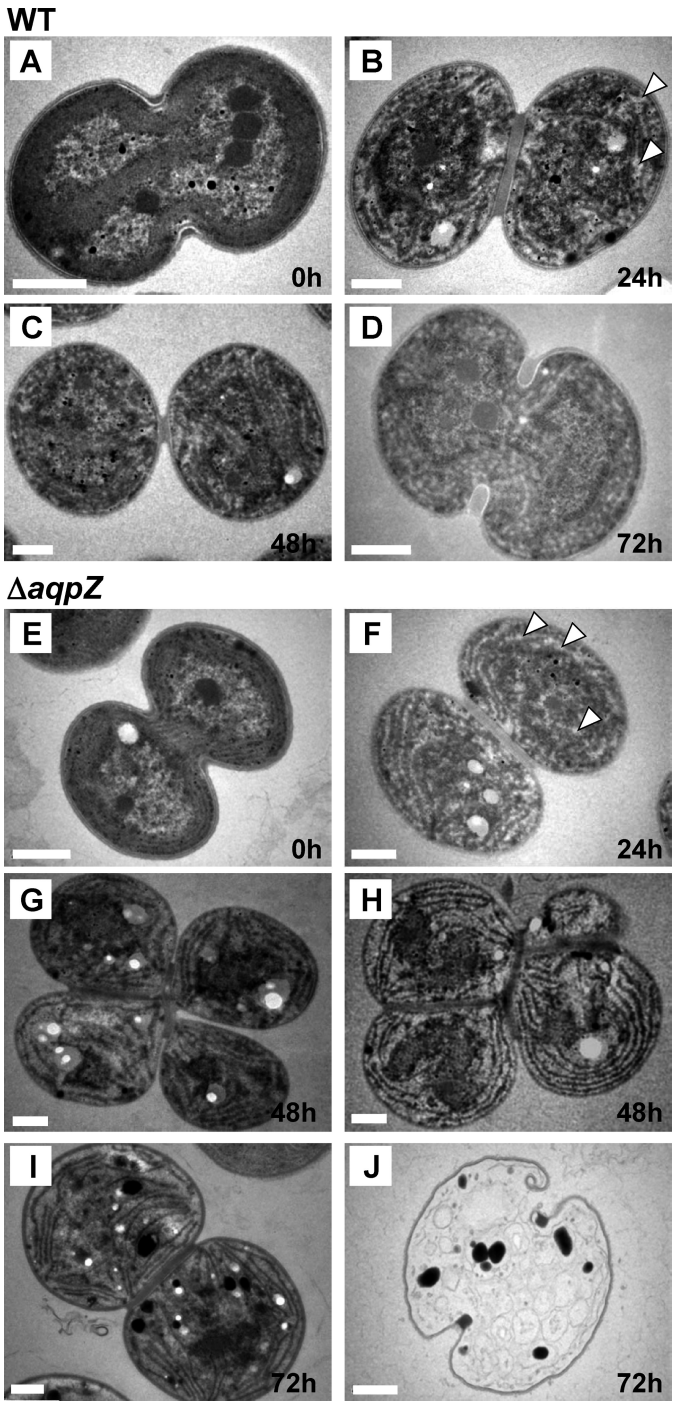

FIGURE 6. **Aberrant morphology of Δ*aqpZ* cells in the presence of glucose.** WT (*A–D*) and Δ*aqpZ* cells (*E–J*) were grown under photomixotrophic conditions for 0, 24, 48, and 72 h. Glycogen granules are indicated by *arrowheads* (*B* and *F*). Incomplete cell division (*G* and *H*), abnormally shaped thylakoid membranes in the cells (*I*), and dead cells (*J*) were observed in the Δ*aqpZ* cell culture. *Bars*, 0.5 μm.

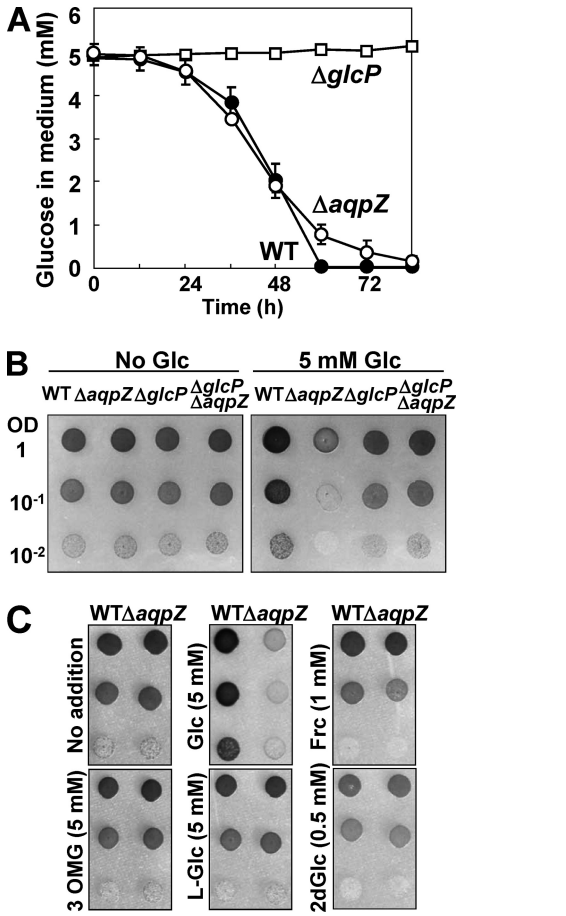

FIGURE 7. **Inhibition of the growth of Δ*aqpZ* cells by glucose was dependent on glucose uptake.** *A*, consumption of glucose in the medium by WT, Δ*aqpZ*, and Δ*glcP* cells. The glucose concentration of the medium (initial concentration was 5 mM) was determined at the times indicated. Data are means ± S.D. (*error bars*) of three independent experiments. *B*, WT, Δ*aqpZ*, Δ*glcP*, and Δ*aqpZ*/Δ*glcP* cells grown on solid medium without (*left*) or with 5 mM glucose (*right*) for 5 days. Each spot consisted of 5 μl of culture diluted to the indicated values of OD_{730}. *C*, WT and Δ*aqpZ* cells grown for 5 days on solid medium containing the indicated concentrations of D-glucose (*Glc*), L-glucose (*L-Glc*), 2-deoxy-glucose (*2dGlc*), 3-*o*-methyl-D-glucose (*3OMG*), or fructose (*Frc*). Each spot consisted of 5 μl of culture diluted to an OD_{730} of 1.0.

Metabolite Profiles of Synechocystis Cells Grown under Photomixotrophic Conditions—To elucidate the impact of loss of *aqpZ* on the metabolite content, we determined the levels of 72 metabolites in extracts of wild-type and Δ*aqpZ* cells (Fig. 10 and supplemental Figs. S2–S5). We applied two-way analysis of variance to find possible interactions between incubation time, intracellular glycogen content, or cell size and metabolite levels (Fig. 10*A* and supplemental Fig. S2). The statistical analysis revealed significant differences in metabolite levels between wild-type and Δ*aqpZ* cells (Fig. 10*B* and supplemental Fig. S2). The culture time-based profiles, which were verified at 48 h under photomixotrophic conditions, showed reduced amounts of isocitrate, citrate, glutamate, sucrose, succinate, ornithine, and spermidine in Δ*aqpZ* cells and a higher abundance of glucose and glucose 6-phosphate, (Fig. 10*B*). Interestingly, the lower level of spermidine, known as a compound that enhances cell proliferation, was correlated with the decrease in cell division of the Δ*aqpZ* cells (51). When we compared the correlation between intracellular glycogen levels or cell sizes and changes in metabolite levels, some of the interaction effects were overlapping (Fig. 10*A*). The overall changes in the levels of metabolites showed that glucose metabolism was inhibited in the Δ*aqpZ* cells (Fig. 10 and supplemental Figs. S3–S6).

Synechocystis AqpZ Does Not Transport Glycerol—One possible explanation for the finding that products of the early steps of glycolysis accumulated in the Δ*aqpZ* mutant would be that

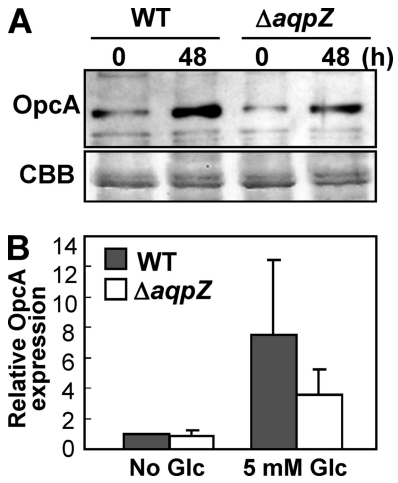

FIGURE 8. **Glucose-induced down-regulation of glucose-6-phosphate dehydrogenase in Δ*aqpZ* cells.** *A*, Western blot analyses of OpcA, a protein essential for glucose-6-phosphate dehydrogenase activity in the pentose phosphate pathway in protein extracts from WT and Δ*aqpZ* cells (*top*). The cells were exposed to 5 mM glucose for 48 h prior to extraction of proteins. Each lane was loaded with 3 μg of protein. Total protein (*CBB*) served as a loading control (*bottom*). *B*, the relative expression level of AqpZ protein was calculated by densitometry in relation to the sample without glucose. Data are mean ± S.D. (*error bars*) of values from three independent experiments.

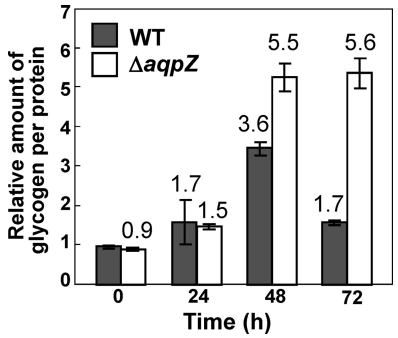

FIGURE 9. **Accumulation of glycogen in Δ*aqpZ* cells under photomixotrophic growth conditions.** WT and Δ*aqpZ* cells were cultured under photomixotrophic conditions (5 mM glucose). The amount of glycogen in the cells was calculated relative to the value for WT (time = 0). Data are means ± S.D. (*error bars*) of values from three independent experiments.

AqpZ has a function in the export of glycerol, one of the products of glucose metabolism. Glycerol transport activity has been shown for some other aquaporins (52, 53). We examined whether AqpZ is able to transport glycerol by using heterologous expression in *E. coli* (supplemental Fig. S7). The *E. coli* MA05 (*glpF*$^-$) or MA06 (*aqpZ*$^-$, *glpF*$^-$) strain complemented with the *E. coli* glycerol transporter gene *glpF* was able to grow on medium containing 2 mM glycerol as the sole carbon source. In contrast, *Synechocystis AqpZ* was not able to rescue the growth defects of strain MA05 or MA06. The same was true for *E. coli AqpZ* and the empty vector (supplemental Fig. S7). These data showed that *Synechocystis* AqpZ did not function as a glycerol transporter in the same way as *E. coli* GlpF.

pH Dependence of ΔaqpZ Cells—Because organic compounds contribute to the cellular pH buffering system (54, 55), the reduced amount of certain metabolites found in Δ*aqpZ* cells (Fig. 10) may result in a disturbance of pH homeostasis in the cells. It has also been reported that glucose affected the pH sensitivity of *Synechocystis* (41, 56). Therefore, we tested the

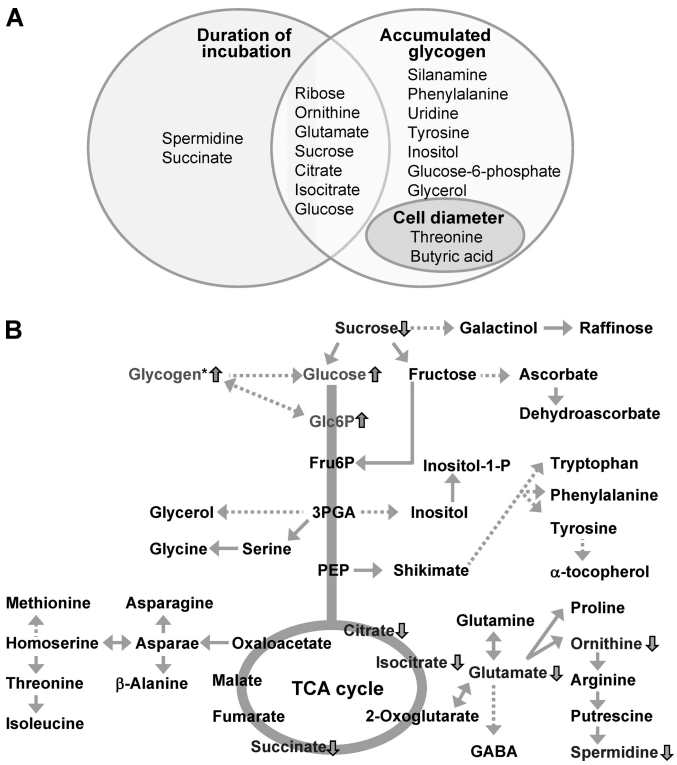

FIGURE 10. **Changes in metabolite levels in Δ*aqpZ* cells in comparison with the WT grown for 48 h under photomixotrophic conditions based on metabolite profiling using GC/TOF-MS.** *A*, Venn diagram of annotated metabolites that showed significant interaction effects with duration of culture, accumulated glycogen, and cell diameter. The corresponding box plots data sets are shown in supplemental Figs. S3–S5. *B*, diagram depicting key steps in glycolysis, the pentose phosphate pathway, the TCA cycle, and related pathways. Increase or decrease of metabolites in the Δ*aqpZ* mutant compared with the wild type is shown as *upward* or *downward arrows*, respectively. The data were derived from the data set shown in supplemental Fig. S2. *3PGA*, 3-phosphoglycerate; *PEP*, phosphoenolpyruvate; *Fru6P*, fructose 6-phosphate; *Glc6P*, glucose 6-phosphate; *GABA*, γ-aminobutyric acid.

growth of Δ*aqpZ* cells in liquid medium with pH values ranging from 6.5 to 10. In medium without glucose, Δ*aqpZ* cells grew identical to the wild type at all pH values tested (Fig. 11, *A* and *B*). Oxygen evolution as a measure of PSII activity was the same for wild-type and Δ*aqpZ* cells in medium without glucose at all pH values tested (Fig. 11*E*). In contrast, under photomixotrophic conditions, when glucose was included in the medium, neither the wild-type nor the Δ*aqpZ* cells grew at pH 6.5 (Fig. 11, *A*, *B*, and *D*). The most significant difference was that the growth rate of the Δ*aqpZ* cells was strongly decreased after 72 h at pH values from 7.5 to 8.5 (Fig. 11, *B* and *D*). Oxygen evolution of the Δ*aqpZ* cells was also strongly decreased at these pH values (Fig. 11, *E* and *F*). These results indicated that hypersensitivity of the Δ*aqpZ* cells to glucose was pH-dependent.

Comparison of the Glucose Sensitivity of Δsll1961 or Δhik31 Mutants with ΔaqpZ Cells—DNA microarray and Northern blotting analysis conducted previously revealed that deletion of *sll1961*, encoding a putative transcription factor, resulted in a decrease in the transcription level of *aqpZ* (57). The *sll1961* mutant was also very sensitive to glucose in the medium (58). The *aqpZ* (*slr2507*) gene is adjacent to *sll1961* but in the opposite orientation on the chromosome (Fig. 12*A*). In addition,

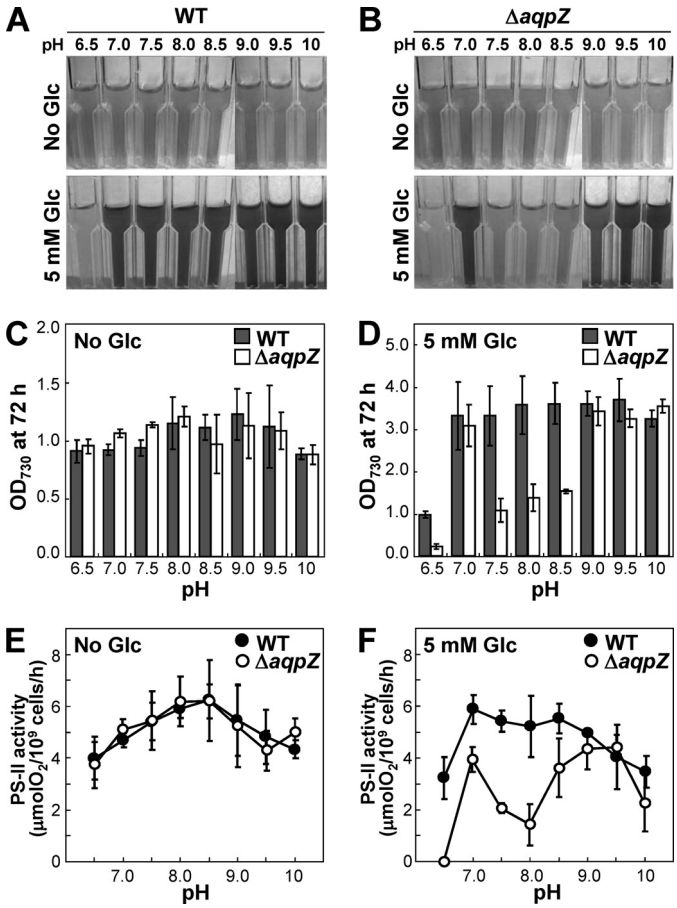

FIGURE 11. **Influence of pH on the glucose sensitivity of the Δ*aqpZ* cells.** *A* and *B*, WT (*A*) and Δ*aqpZ* cells (*B*) were grown for 72 h at 30 °C under photoautotrophic or photomixotrophic (5 mM glucose) conditions in media with different initial pH values. Aliquots of each culture were photographed. *C* and *D*, the OD_{730} of the cultures was measured after 72 h of growth. *E* and *F*, PSII-dependent oxygen evolution from the cells was determined after 48 h. *Error bars*, S.D.

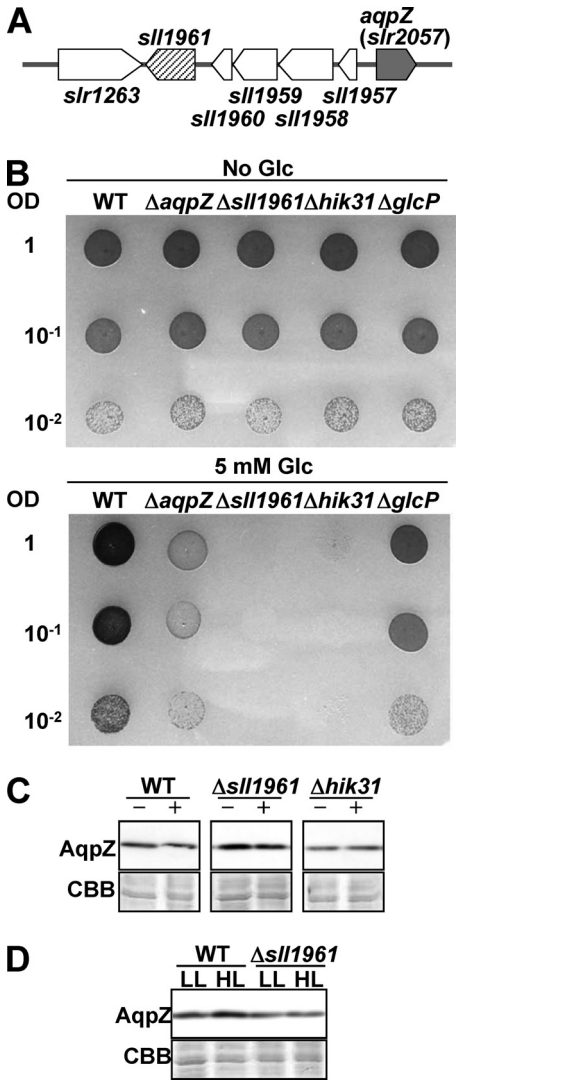

FIGURE 12. **Influence of the putative positive transcription regulator, *sll1961*, on *apqZ* expression.** *A*, the position of *sll1961* and *aqpZ* in the chromosomal DNA. *B*, WT, Δ*aqpZ*, Δ*sll1961*, Δ*hik31*, and Δ*glcP* cells were grown to mid-exponential phase and spotted onto solid medium without (*top*) or with 5 mM glucose (*bottom*). Each spot consisted of 5 μl of liquid culture diluted to an OD_{730} of 1, 0.1, or 0.01. Plates were incubated at 30 °C for 5 days. *C*, Western blot analysis of AqpZ protein in WT, Δ*sll1961*, or Δ*hik31* cells grown in medium containing 5 mM glucose (+) or no glucose (−). *D*, Western blot analysis of AqpZ protein in WT and Δ*sll1961* cells grown in medium without glucose under low light (*LL*) or high light (*HL*) conditions.

inactivation of the *hik31* gene, encoding a sensory histidine kinase, also suppressed cell growth in the presence of glucose (44). We compared the phenotypes of these two mutants with that of the Δ*aqpZ* cells (Fig. 12*B*). Both mutants, Δ*sll1961* and Δ*hik31*, exhibited more severe growth inhibition in the presence of glucose than the Δ*aqpZ* cells. Immunoblot analysis showed that in the presence of glucose in the medium, the amount of AqpZ protein was slightly decreased in the Δ*sll1961* cells but unchanged in the Δ*hik31* cells (Fig. 12*C*). High light conditions increased the amount of AqpZ protein in the wild type, which was consistent with the results of the DNA microarray (57). No increase in AqpZ protein expression level in high light conditions was seen in the Δ*sll1961* mutant (Fig. 12*D*). These data suggest that *sll1961* may partially regulate the expression of AqpZ protein.

DISCUSSION

Loss of function of the plasma membrane-localized aquaporin AqpZ made *Synechocystis* cells unable to grow in medium containing glucose. Δ*aqpZ* cells showed aberrant cellular morphology and were affected in cell division (Figs. 2 and 6). This glucose sensitivity was dependent on glucose uptake, and in the absence of a functioning glucose transporter, glucose in the medium had no negative effect on Δ*aqpZ* cells (Fig. 7). This is compelling evidence because not much information on the phenotypes of aquaporin-deficient strains is available (6). *Synechocystis* uses the degradation of glucose into smaller molecules via the pentose phosphate pathway and glycolysis to increase intracellular osmolarity (44, 50). Consistent with this, both wild-type and Δ*aqpZ* cells grown on medium with glucose swelled more compared with cells grown in the absence of glucose (Fig. 5). The Δ*aqpZ* cells were larger in size than the wild type, which may be the result of a decrease in water permeability due to the loss of AqpZ function. Based on OpcA protein expression (Fig. 8) and metabolite profiling of the Δ*aqpZ* cells (Fig. 10 and supplemental Figs. S3–S6), glucose in the medium led to a decrease in glucose degradation and to enhanced glycogen synthesis, most likely to limit swelling of the cells (Fig. 9).

This is in agreement with previous reports that the glycogen content was elevated or that glucose catabolism was impaired in *Synechocystis* when cells were exposed to excess glucose (29, 41, 48, 59). The observed decrease in the content of spermidine, a compound known to be involved in the enhancement of cell division, is consistent with decreased cell growth after glucose addition to the medium (51) (Fig. 10).

Water transport across the membrane is coordinated with the transport of various solutes, which are in turn closely associated with the formation of proton motive force consisting of pH gradient and membrane potential across the membrane (12, 60). The potassium transport system, consisting of Ktr-type transporters and potassium channels, and the sodium extrusion system of Na^+/H^+ antiporters in the plasma membrane of *Synechocystis* function to control the turgor pressure and the electrochemical membrane potential in response to extracellular or intracellular environmental changes (21, 61–69). The immediate adjustment to changes of membrane potential or cellular osmolarity requires fast water flux across the plasma membrane in response to the conversion of glucose into various types of molecules through the carbon metabolism pathway. In addition, intermediate metabolites like citrate and malate derived from glucose through glycolysis and the TCA cycle are known to be important for regulation of pH homeostasis, ΔpH, and the proton motive force (70). *Synechocystis* mutants impaired in tocopherol biosynthesis, which is an antioxidant small metabolite, are also affected in their pH dependence (41). The Δ*aqpZ* mutant was sensitive to pH values between pH 7.5 and pH 8.5 in glucose-containing medium and showed inactivation of PSII (Fig. 11). This may be the result of changed levels of metabolites detected in the Δ*aqpZ* cells.

We analyzed potential effects on carbon metabolism by GC/TOF-MS profiling of Δ*aqpZ* and wild-type cells and compared their metabolite contents. Metabolite profiling data were used to analyze possible interactions between glycogen content, cell size, and metabolite levels (supplemental Figs. S4–S6). The content of glucose 6-phosphate and glucose increased in the Δ*aqpZ* cells after 48 h of growth, whereas the levels of products of the tricarboxylic acid cycle and some amino acids remained unchanged or were lower compared with the wild type. This is in agreement with the finding that the influx of glucose into the pentose phosphate pathway was reduced (Fig. 8). Consistent with this, statistical analyses showed that the Δ*aqpZ* cells overall contained lower levels of metabolites compared with the wild type (Fig. 10 and supplemental Figs. S3–S6). The reduction in the amount of metabolites derived from the degradation of glucose prevented an increase of the intracellular osmolarity and promoted glycogen synthesis in the cells.

Fujimori *et al.* (57) isolated the *sll1961* mutant based on its hypersensitivity to high light conditions. In a subsequent study, the same group found that glucose in the medium reduced the growth of the *sll1961* mutant (58). DNA microarray analysis revealed that loss of function of *sll1961* resulted in decreased expression of *aqpZ* at the transcriptional level, indicating that *sll1961* is a positive transcription regulator for *aqpZ* gene expression. This functional relationship between *sll1961* and *aqpZ* is further supported by their adjacent position in the *Synechocystis* genome. We compared the sensitivity of the Δ*sll1961* and the Δ*aqpZ* mutant to glucose and the level of AqpZ protein in cells grown without and with glucose and found some evidence for a regulatory role of *sll1961* on *aqpZ* expression (Fig. 12). However, because loss of function of *sll1961* did not result in a lack of AqpZ protein, we concluded that *sll1961* only had a limited role in *aqpZ* expression.

Like other aquaporins, AqpZ can mediate both inward and outward water flow (Fig. 1) (71). Because the genome of *Synechocystis* PCC 6803 contains a single gene encoding an aquaporin, *aqpZ*, and our results showed that AqpZ resides in the plasma membrane (Fig. 2 and supplemental Fig. S1), this leads to the following questions. Is AqpZ the only water transport system? What is the water permeation route across the thylakoid membrane? The detailed structural analysis of potassium channels revealed that they allow the passage of water molecules through the conducting pore (72). Considering these findings, we predict that other membrane proteins in addition to AqpZ may conduct the diffusion of water across membranes.

It is also possible that AqpZ may be required for the transport of products synthesized during the process of glucose metabolism. Many aquaporins have been documented to act as facilitators of water, glycerol, peroxide, CO_2, and other small, uncharged, ubiquitous molecules (11, 12). We therefore tested the possibility that glycerol may be able to pass through AqpZ by heterologous expression of *aqpZ* in *E. coli glpF* mutants but did not observe glycerol transport activity (supplemental Fig. S7). It cannot be excluded that passage of small metabolites through AqpZ may be required in order to discharge cytotoxic compounds from cells growing on glucose-containing media. This would explain why cells lacking AqpZ were hypersensitive to glucose and were larger than the wild type in the presence of 5 mM glucose (Fig. 5).

In summary, our efforts in characterizing Δ*aqpZ* cells under photomixotrophic conditions have yielded new insights into the role of aquaporin in glucose metabolism in *Synechocystis*. Loss of function of *aqpZ* resulted in a down-regulation of glucose hydrolysis after glucose addition into the medium and an increase of glycogen synthesis. Therefore, in addition to its role as a water channel, AqpZ plays a role in regulating cell volume, macronutrient homeostasis, and cell division under photomixotrophic conditions.

Acknowledgments—We thank Tatsuo Omata (Nagoya University) for the anti-NrtA antibodies, Eva-Mari Aro (University of Turku) and Teruo Ogawa (Nagoya University) for the antibodies against NdhD3 and NdhF3, John C. Meeks (University of California, Davis) for the anti-OpcA antibodies, Iwane Suzuki (Tsukuba University) for the Δhik31 cells, Makoto Kobayashi and Hitomi Otsuki (RIKEN Plant Science Center) for metabolomics analysis, Takako Kawai (RIKEN Plant Science Center) for performing electron microscopy, and Anke Reinders (University of Minnesota) for critical reading of the manuscript.

REFERENCES

1. Preston, G. M., Carroll, T. P., Guggino, W. B., and Agre, P. (1992) *Science* **256,** 385–387
2. Agre, P., and Kozono, D. (2003) *FEBS Lett.* **555,** 72–78
3. Czempinski, K., Frachisse, J. M., Maurel, C., Barbier-Brygoo, H., and Mu-

eller-Roeber, B. (2002) *Plant J.* **29,** 809–820
4. Maurel, C., Reizer, J., Schroeder, J. I., and Chrispeels, M. J. (1993) *EMBO J.* **12,** 2241–2247
5. Shapiguzov, A., Lyukevich, A. A., Allakhverdiev, S. I., Sergeyenko, T. V., Suzuki, I., Murata, N., and Los, D. A. (2005) *Microbiology* **151,** 447–455
6. Tanghe, A., Van Dijck, P., and Thevelein, J. M. (2006) *Trends Microbiol.* **14,** 78–85
7. Calamita, G., Kempf, B., Bonhivers, M., Bishai, W. R., Bremer, E., and Agre, P. (1998) *Proc. Natl. Acad. Sci. U.S.A.* **95,** 3627–3631
8. Soupene, E., King, N., Lee, H., and Kustu, S. (2002) *J. Bacteriol.* **184,** 4304–4307
9. Delamarche, C., Thomas, D., Rolland, J. P., Froger, A., Gouranton, J., Svelto, M., Agre, P., and Calamita, G. (1999) *J. Bacteriol.* **181,** 4193–4197
10. Hill, A. E., Shachar-Hill, B., and Shachar-Hill, Y. (2004) *J. Membr. Biol.* **197,** 1–32
11. Yasui, M., Hazama, A., Kwon, T. H., Nielsen, S., Guggino, W. B., and Agre, P. (1999) *Nature* **402,** 184–187
12. Maurel, C. (2007) *FEBS Lett.* **581,** 2227–2236
13. Williams, J. G. K. (1988) *Methods Enzymol.* **167,** 776–778
14. Anderson, S. L., and McIntosh, L. (1991) *J. Bacteriol.* **173,** 2761–2767
15. Uozumi, N., Gassmann, W., Cao, Y., and Schroeder, J. I. (1995) *J. Biol. Chem.* **270,** 24276–24281
16. Ma, T., Frigeri, A., Skach, W., and Verkman, A. S. (1993) *Biochem. Biophys. Res. Commun.* **197,** 654–659
17. Chakrabarti, N., Roux, B., and Pomès, R. (2004) *J. Mol. Biol.* **343,** 493–510
18. Liu, K., Kozono, D., Kato, Y., Agre, P., Hazama, A., and Yasui, M. (2005) *Proc. Natl. Acad. Sci. U.S.A.* **102,** 2192–2197
19. Meetam, M., Keren, N., Ohad, I., and Pakrasi, H. B. (1999) *Plant Physiol.* **121,** 1267–1272
20. Norling, B., Zak, E., Andersson, B., and Pakrasi, H. (1998) *FEBS Lett.* **436,** 189–192
21. Tsunekawa, K., Shijuku, T., Hayashimoto, M., Kojima, Y., Onai, K., Morishita, M., Ishiura, M., Kuroda, T., Nakamura, T., Kobayashi, H., Sato, M., Toyooka, K., Matsuoka, K., Omata, T., and Uozumi, N. (2009) *J. Biol. Chem.* **284,** 16513–16521
22. Omata, T. (1995) *Plant Cell Physiol.* **36,** 207–213
23. Ohkawa, H., Price, G. D., Badger, M. R., and Ogawa, T. (2000) *J. Bacteriol.* **182,** 2591–2596
24. Zhang, P., Battchikova, N., Jansen, T., Appel, J., Ogawa, T., and Aro, E. M. (2004) *Plant Cell* **16,** 3326–3340
25. Stanier, R. Y., Kunisawa, R., Mandel, M., and Cohen-Bazire, G. (1971) *Bacteriol. Rev.* **35,** 171–205
26. Sundaram, S., Karakaya, H., Scanlan, D. J., and Mann, N. H. (1998) *Microbiology* **144,** 1549–1556
27. Hagen, K. D., and Meeks, J. C. (2001) *J. Biol. Chem.* **276,** 11477–11486
28. Toyooka, K., Moriyasu, Y., Goto, Y., Takeuchi, M., Fukuda, H., and Matsuoka, K. (2006) *Autophagy* **2,** 96–106
29. Osanai, T., Kanesaki, Y., Nakano, T., Takahashi, H., Asayama, M., Shirai, M., Kanehisa, M., Suzuki, I., Murata, N., and Tanaka, K. (2005) *J. Biol. Chem.* **280,** 30653–30659
30. Forchhammer, K., and Tandeau de Marsac, N. (1995) *J. Bacteriol.* **177,** 2033–2040
31. Datsenko, K. A., and Wanner, B. L. (2000) *Proc. Natl. Acad. Sci. U.S.A.* **97,** 6640–6645
32. Froger, A., Rolland, J. P., Bron, P., Lagrée, V., Le Cahérec, F., Deschamps, S., Hubert, J. F., Pellerin, I., Thomas, D., and Delamarche, C. (2001) *Microbiology* **147,** 1129–1135
33. Jonsson, P., Gullberg, J., Nordström, A., Kusano, M., Kowalczyk, M., Sjöström, M., and Moritz, T. (2004) *Anal. Chem.* **76,** 1738–1745
34. Jonsson, P., Johansson, E. S., Wuolikainen, A., Lindberg, J., Schuppe-Koistinen, I., Kusano, M., Sjöström, M., Trygg, J., Moritz, T., and Antti, H. (2006) *J. Proteome Res.* **5,** 1407–1414
35. Kusano, M., Fukushima, A., Kobayashi, M., Hayashi, N., Jonsson, P., Moritz, T., Ebana, K., and Saito, K. (2007) *J. Chromatogr. B Analyt. Technol. Biomed. Life Sci.* **855,** 71–79
36. Kusano, M., Fukushima, A., Arita, M., Jonsson, P., Moritz, T., Kobayashi, M., Hayashi, N., Tohge, T., and Saito, K. (2007) *BMC Syst. Biol.* **1,** 53
37. Schauer, N., Steinhauser, D., Strelkov, S., Schomburg, D., Allison, G., Moritz, T., Lundgren, K., Roessner-Tunali, U., Forbes, M. G., Willmitzer, L., Fernie, A. R., and Kopka, J. (2005) *FEBS Lett.* **579,** 1332–1337
38. Kopka, J., Schauer, N., Krueger, S., Birkemeyer, C., Usadel, B., Bergmüller, E., Dörmann, P., Weckwerth, W., Gibon, Y., Stitt, M., Willmitzer, L., Fernie, A. R., and Steinhauser, D. (2005) *Bioinformatics* **21,** 1635–1638
39. Redestig, H., Fukushima, A., Stenlund, H., Moritz, T., Arita, M., Saito, K., and Kusano, M. (2009) *Anal. Chem.* **81,** 7974–7980
40. Smyth, G. K. (2004) *Stat. Appl. Genet. Mol. Biol.* **3,** Article3
41. Sakuragi, Y., Maeda, H., Dellapenna, D., and Bryant, D. A. (2006) *Plant Physiol.* **141,** 508–521
42. Schmetterer, G. R. (1990) *Plant Mol. Biol.* **14,** 697–706
43. Zhang, C. C., Jeanjean, R., and Joset, F. (1998) *FEMS Microbiol. Lett.* **161,** 285–292
44. Kahlon, S., Beeri, K., Ohkawa, H., Hihara, Y., Murik, O., Suzuki, I., Ogawa, T., and Kaplan, A. (2006) *Microbiology* **152,** 647–655
45. Yang, C., Hua, Q., and Shimizu, K. (2002) *Metab. Eng.* **4,** 202–216
46. Yang, C., Hua, Q., and Shimizu, K. (2002) *Appl. Microbiol. Biotechnol.* **58,** 813–822
47. Knowles, V. L., and Plaxton, W. C. (2003) *Plant Cell Physiol.* **44,** 758–763
48. Singh, A. K., and Sherman, L. A. (2005) *J. Bacteriol.* **187,** 2368–2376
49. Lee, S., Ryu, J. Y., Kim, S. Y., Jeon, J. H., Song, J. Y., Cho, H. T., Choi, S. B., Choi, D., de Marsac, N. T., and Park, Y. I. (2007) *Plant Physiol.* **145,** 1018–1030
50. Takahashi, H., Uchimiya, H., and Hihara, Y. (2008) *J. Exp. Bot.* **59,** 3009–3018
51. Igarashi, K., and Kashiwagi, K. (2006) *J. Biochem.* **139,** 11–16
52. Hibuse, T., Maeda, N., Nagasawa, A., and Funahashi, T. (2006) *Biochim. Biophys. Acta* **1758,** 1004–1011
53. Wintour, E. M., and Henry, B. A. (2006) *Trends Endocrinol. Metab.* **17,** 77–78
54. Daeschel, M. A. (1988) *Appl. Environ. Microbiol.* **54,** 1627–1629
55. Korithoski, B., Krastel, K., and Cvitkovitch, D. G. (2005) *J. Bacteriol.* **187,** 4451–4456
56. Ryu, J. Y., Song, J. Y., Lee, J. M., Jeong, S. W., Chow, W. S., Choi, S. B., Pogson, B. J., and Park, Y. I. (2004) *J. Biol. Chem.* **279,** 25320–25325
57. Fujimori, T., Higuchi, M., Sato, H., Aiba, H., Muramatsu, M., Hihara, Y., and Sonoike, K. (2005) *Plant Physiol.* **139,** 408–416
58. Ozaki, H., Ikeuchi, M., Ogawa, T., Fukuzawa, H., and Sonoike, K. (2007) *Plant Cell Physiol.* **48,** 451–458
59. Osanai, T., Imamura, S., Asayama, M., Shirai, M., Suzuki, I., Murata, N., and Tanaka, K. (2006) *DNA Res.* **13,** 185–195
60. Tournaire-Roux, C., Sutka, M., Javot, H., Gout, E., Gerbeau, P., Luu, D. T., Bligny, R., and Maurel, C. (2003) *Nature* **425,** 393–397
61. Mikkat, S., Milkowski, C., and Hagemann, M. (2000) *Plant Cell Environ.* **23,** 549–559
62. Inaba, M., Sakamoto, A., and Murata, N. (2001) *J. Bacteriol.* **183,** 1376–1384
63. Elanskaya, I. V., Karandashova, I. V., Bogachev, A. V., and Hagemann, M. (2002) *Biochemistry* **67,** 432–440
64. Berry, S., Esper, B., Karandashova, I., Teuber, M., Elanskaya, I., Rögner, M., and Hagemann, M. (2003) *FEBS Lett.* **548,** 53–58
65. Matsuda, N., Kobayashi, H., Katoh, H., Ogawa, T., Futatsugi, L., Nakamura, T., Bakker, E. P., and Uozumi, N. (2004) *J. Biol. Chem.* **279,** 54952–54962
66. Matsuda, N., and Uozumi, N. (2006) *Biosci. Biotechnol. Biochem.* **70,** 273–275
67. Zulkifli, L., and Uozumi, N. (2006) *J. Bacteriol.* **188,** 7985–7987
68. Zulkifli, L., Akai, M., Yoshikawa, A., Shimojima, M., Ohta, H., Guy, H. R., and Uozumi, N. (2010) *J. Bacteriol.* **192,** 5063–5070
69. Zanetti, M., Teardo, E., La Rocca, N., Zulkifli, L., Checchetto, V., Shijuku, T., Sato, Y., Giacometti, G. M., Uozumi, N., Bergantino, E., and Szabò, I. (2010) *PLoS One* **5,** e10118
70. Bandell, M., Ansanay, V., Rachidi, N., Dequin, S., and Lolkema, J. S. (1997) *J. Biol. Chem.* **272,** 18140–18146
71. Azad, A. K., Sato, R., Ohtani, K., Sawa, Y., Ishikawa, T., and Shibata, H. (2011) *Plant Sci.* **180,** 375–382
72. Doyle, D. A., Morais Cabral, J., Pfuetzner, R. A., Kuo, A., Gulbis, J. M., Cohen, S. L., Chait, B. T., and MacKinnon, R. (1998) *Science* **280,** 69–77